

# A Comparison Study of Photocatalytic Activity of $\text{Fe}_3\text{O}_4/\text{TiO}_2$ and $\text{Ag}/\text{TiO}_2$ on the Degradation of 2, 4-Dichlorophenol

Narjes Esmaeili<sup>1, a)</sup> Azadeh Ebrahimian Pirbazari<sup>2, b)</sup> Ziba Khodaei<sup>3, c)</sup>

<sup>1</sup>M. Sc. Student, Caspian Faculty of Engineering, College of Engineering, University of Tehran, P.O. Box 43841-119, Rezvanshahr 43861-56387, Iran,

<sup>2</sup>Assistant Professor, Fouman Faculty of Engineering, College of Engineering, University of Tehran, P.O. Box 43515-1155, Fouman 43516-66456, Iran.

<sup>3</sup>Assistant Professor, University of Applied Science and Technology, P.O. Box 41635-3697, Guilan, Iran,

<sup>a)</sup> narjes.esmaeili@ut.ac.ir

<sup>b)</sup> Corresponding author: aebrahimian@ut.ac.ir

<sup>c)</sup> zibakhodaei@uast.ac.ir

**Abstract** In this work, pure  $\text{TiO}_2$  and binary nanocomposites of  $\text{Fe}_3\text{O}_4/\text{TiO}_2$  and  $\text{Ag}/\text{TiO}_2$  were synthesized in order to improve photocatalytic performance of these samples for degradation of 2, 4-dichlorophenol (2, 4-DCP) as an organic pollutant. A range of analytical techniques including XRD, DRS, SEM/EDX, and elemental mapping were employed to reveal the crystal structure, morphology and property of the nanocomposites. XRD data demonstrated that the prepared samples are purely in  $\text{TiO}_2$  anatase phase and cubic spinel  $\text{Fe}_3\text{O}_4$  exist in the synthesized nanocomposite. We calculated the  $\text{TiO}_2$  crystal size from XRD patterns, in the range of 8.35-11.09 nm. The presence of Ag, Fe, O, and Ti atoms in the synthesized nanocomposites was confirmed by SEM/EDX. We obtained 30.43, 32.02 and 42.40 % degradation of 2, 4-DCP (100 ml 2, 4-DCP 40 ppm and 0.01 g catalyst) for pure  $\text{TiO}_2$ ,  $\text{Fe}_3\text{O}_4/\text{TiO}_2$  and  $\text{Ag}/\text{TiO}_2$ , respectively, after 180 min of irradiation under visible light. Similar conditions were employed for 2, 4-DCP degradation under UV irradiation, we obtained 53.05, 51.00 and 71.50 % degradation of 2, 4-DCP pure  $\text{TiO}_2$ ,  $\text{Fe}_3\text{O}_4/\text{TiO}_2$  and  $\text{Ag}/\text{TiO}_2$ , respectively. Thus, the synthesized binary nanocomposites exhibited higher photocatalytic activity compared to pure  $\text{TiO}_2$  under visible light.

## INTRODUCTION

World's population growth and drinking water scarcity has made drinking water supplementation, one of the fundamental problems of today's world. Therefore, water recycling will provide access to a suitable source for various uses. Recently, advanced oxidation processes (AOPs) have been proposed as a wastewater treatment solution. Among advanced oxidation processes, heterogeneous photocatalytic processes have been used as a successful method for the decomposition of various organic pollutants. Photocatalysts are environmental cleaners that can degrade many environmental pollutants through oxidation by using sunlight or artificial light, especially ultraviolet light. Titanium dioxide ( $\text{TiO}_2$ ) is one of the photocatalysts that has been used to degrade organic pollutants.  $\text{TiO}_2$  is an ideal photocatalyst with non-toxic nature, high oxidizing properties under UV radiation and low cost, which is stable under various reaction conditions and is also environment friendly [1].

There are two distinct defects in the performance of  $\text{TiO}_2$  for the destruction of environmental pollutants. The first is the high energy of its separation band (3.2 eV), which requires UV radiation to generate the electron-cavity pair, but UV radiation forms only about 4% of the sun's emission. In order to utilize a larger part of the radiation emitted from the sun, it is necessary to make special changes in this semiconductor system. The presence of metals such as silver at  $\text{TiO}_2$  surface would reduce the separation band energy and expand its absorption spectrum towards the visible light region. The presence of these metals decreases recombination rate of electron-cavity pair and also increases the

free radicals formation rate [2]. The second defect is the recycling of nano-sized photocatalysts, which is very difficult and costly. An operational solution for photocatalyst recycling is magnetizing  $\text{TiO}_2$  by  $\text{Fe}_3\text{O}_4$  so that it can be separated and reused by employment of an external magnetic field [3]. In this study,  $(\text{Ag}/\text{TiO}_2)$  and  $(\text{Fe}_3\text{O}_4/\text{TiO}_2)$  binary nanocomposites as well as pure  $\text{TiO}_2$  will be synthesized by sol-gel method. The synthesized samples will be identified with various techniques such as DRS, SEM/EDX and XRD, and eventually photocatalysts are used for photocatalytic degradation of 2, 4-dichlorophenol as an organic pollutants both under visible and ultraviolet light.

## EXPERIMENTAL

### Materials

$\text{FeCl}_3 \cdot 6\text{H}_2\text{O}$  (Merck No. 103943),  $\text{FeSO}_4 \cdot 7\text{H}_2\text{O}$  (Merck No. 103965) were used for synthesis of  $\text{Fe}_3\text{O}_4$  nanoparticles (NPs). Tetraisopropylorthotitanat (TIP) (Merck No. 8.21895), anhydrous ethanol, ammonia, and High-purity 2, 4-DCP, 98%, (Merck No. 803774) was used as a probe molecule for photocatalytic tests were purchased from Merck Company. Silver nitrate ( $\text{AgNO}_3$ ), 99.9%, was supplied by (Merck, No.101510), Acetic acid ( $\text{CH}_3\text{COOH}$ ), 99.9% (Merck No. 1.00063). All the reagents were of analytic grade and used without further purification. Double distilled water was used for preparation of all aqueous solutions.

### Preparation of $\text{Fe}_3\text{O}_4$ and $\text{TiO}_2$ NPs

We synthesized  $\text{Fe}_3\text{O}_4$  nanoparticles by chemical precipitation technique according to Mentioned procedure in ref [4] and for synthesis of  $\text{TiO}_2$ , the method reported in reference [5] will be used with some modifications. Subsequently, the obtained nanoparticles identified by various analysis.

### Synthesis of binary $(\text{Fe}_3\text{O}_4/\text{TiO}_2)$ and $(\text{Ag}/\text{TiO}_2)$ nanocomposites

$(\text{Fe}_3\text{O}_4/\text{TiO}_2)$  nanocomposites Synthesis: We mixed 0.1 g of the  $\text{Fe}_3\text{O}_4$  nanoparticles with 4 ml of titanium isopropoxide (TIP) (as a titanium source) and 70 ml of water-free ethanol and placed it in an ultrasonic bath for one hour (Solution A). Solution B prepared by mixing 3 ml of acetic acid and 90 ml of distilled water. Then solution B was added to solution A, stirred at 50 °C for 30 min. Finally, after cooling to room temperature, we separate the synthesized solid from the suspension by centrifugation. Rinsed with ethanol and dried for 12 h at 60 °C. For the final step, the obtained solid is heated under atmospheric pressure at 300 °C for one hour.

$(\text{Ag}/\text{TiO}_2)$  nanocomposites Synthesis: 1 g of  $\text{TiO}_2$  is spread in 20 ml of deionized water by ultrasound waves and subsequently, 1 ml of  $\text{AgNO}_3$ , 100 mM, was slowly added to mixture. The solution was stirred at room temperature for 30 min, then 1 ml of  $\text{Na}_2\text{CO}_3$  (1% w / v), was slowly added. The slurry was filtered and dried at room temperature [6].

### Characterization

The XRD patterns were recorded on a Siemens, D5000 (Germany). The morphology of the prepared samples were characterized using scanning electron microscope (SEM) (Vegall-Tescan Company) equipped with an energy dispersive X-ray (EDX). The diffuse reflectance UV-Vis spectra (DRS) of the samples were recorded by an Ava Spec-2048TEC spectrometer.

### Photocatalytic degradation of 2, 4-DCP

In a typical run, the suspension containing 10 mg photocatalyst and 100 mL aqueous solution of 2, 4-DCP (40 mg/L) was stirred first in the dark for 10 min to establish adsorption/desorption equilibrium. Irradiation experiments were carried out in a self-built reactor for 180min irradiation. UV illumination was performed with a 400 W Kr lamp (Osram). A visible (Halogen, ECO OSRAM, 500W) lamp was used as irradiation source. At certain intervals, small aliquots (2 mL) were withdrawn and filtered to remove the photocatalyst particles. These aliquots were used for monitoring the degradation progress, with Rayleigh UV-2601 UV/VIS spectrophotometer ( $\lambda_{\text{max}} = 227\text{nm}$ ).

## RESULT AND DISCUSSION

### X-ray diffraction analysis

Figure 1. A shows the X-ray diffraction pattern of the synthesized  $\text{Fe}_3\text{O}_4$  nanoparticles in the present study. The diffractions at  $2\theta = 30.2^\circ, 35.6^\circ, 43.5^\circ, 54.3^\circ, 57.4^\circ$  and  $63.1^\circ$  are observed, which are related to the cubic spinel structure of  $\text{Fe}_3\text{O}_4$ , reported by JCPDS reference number 0629-9, thus synthesis of magnetic nanoparticles is confirmed [7].

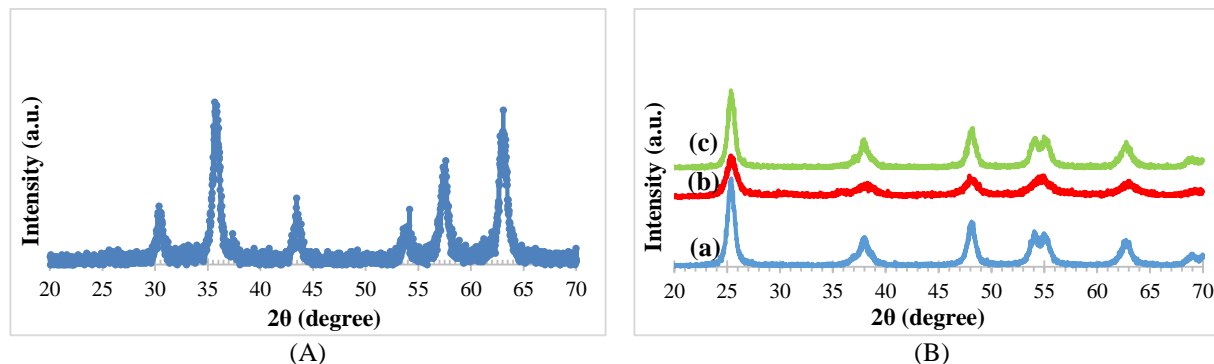


FIGURE 1. XRD patterns of A)  $\text{Fe}_3\text{O}_4$ , B) a)  $\text{TiO}_2$ , b)  $\text{Fe}_3\text{O}_4/\text{TiO}_2$  and c)  $\text{Ag}/\text{TiO}_2$

Figure 1. B shows the XRD patterns of the pure  $\text{TiO}_2$  and binary nanocomposite. All the observed diffractions are related to the anatase phase according to the reference (PDF 24-1272) [8]. The reason for the low intensity of  $\text{Fe}_3\text{O}_4$  nanoparticles and silver atoms diffraction is that they are very small in comparison to  $\text{TiO}_2$ , and because of the high  $\text{TiO}_2$  crystallinity, most of the  $\text{Fe}_3\text{O}_4$  diffraction is not visible.

The size of the  $\text{TiO}_2$  crystal was calculated using first diffraction width and Scherrer's equation. Which varies between 8.35 to 11.09 nm [9].

$$D_{(hkl)} = 0.9\lambda / \beta \cos \theta$$

In this equation,  $D$  ( $hkl$ ) is the crystal size based on Miller's index (101),  $\lambda$  is the wavelength of the X-ray,  $\beta$  is the width of the peak at half of its height, and  $\theta$  is the Bragg's angle for the desired diffraction. Also, to calculate the parameters ( $a = b \neq c$ ), 101 crystalline location of anatase phase is used from the following equation.

$$1/d^2 = (h^2 + k^2)/a^2 + l^2/c^2$$

In this equation,  $D$ , the distance between neighboring places, is calculated by Bragg's law

$$D_{(hkl)} = \lambda / 2 \sin \theta$$

To calculate  $a = b$  and  $c$ , respectively, the angles of the third (2 0 0) and first (1 0 1) diffractions of the anatase phase are used respectively [10]. Table 1 shows the unit cell parameters and volume for the anatase phase  $\text{TiO}_2$  in the synthesized samples and confirmed the formation of pure anatase phase.

TABLE 1. Phase, crystal size and lattice parameters of the prepared samples

Sample	Phase	Crystal size (nm)	a=b (Å)	c (Å)	Cell volume (Å <sup>3</sup> )
$\text{TiO}_2$	Anatase	10.38	3.77	9.59	136.30
$\text{Fe}_3\text{O}_4/\text{TiO}_2$	Anatase	7.11	3.79	9.37	134.87
$\text{Ag}/\text{TiO}_2$	Anatase	8.14	3.77	9.76	138.71

### FESEM/EDX analysis

In order to investigate the surface morphology of the synthesized samples, FESEM studies were performed. The SEM images of pure  $\text{TiO}_2$ ,  $\text{Fe}_3\text{O}_4/\text{TiO}_2$  and  $\text{Ag}/\text{TiO}_2$  samples are shown in Fig. 2. The EDX results were used to examine the elemental composition of the pure  $\text{TiO}_2$ ,  $\text{Fe}_3\text{O}_4/\text{TiO}_2$  and  $\text{Ag}/\text{TiO}_2$  nanocomposites (Fig. 3 and Table 2).

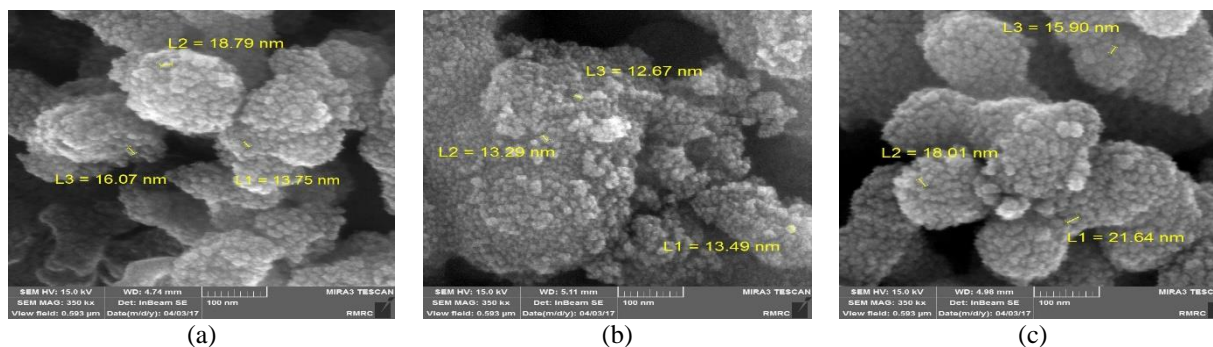


FIGURE 2. FESEM images of a)  $\text{TiO}_2$ , b)  $\text{Fe}_3\text{O}_4/\text{TiO}_2$  and c)  $\text{Ag}/\text{TiO}_2$

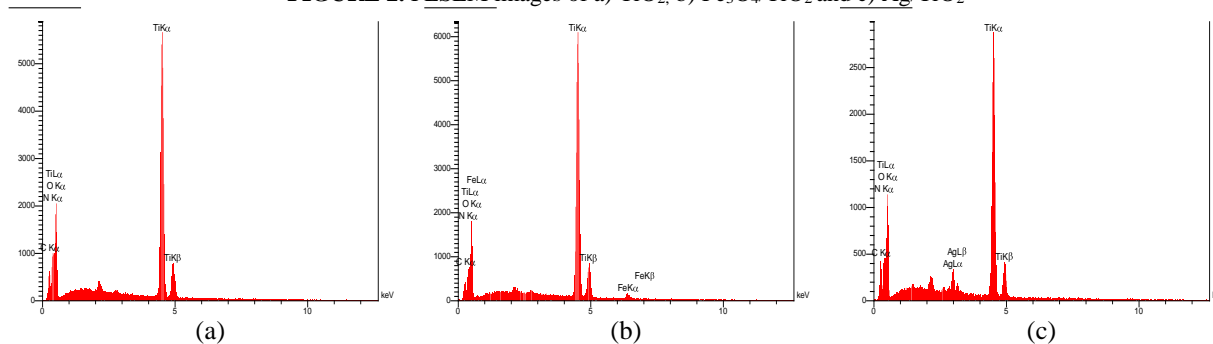


FIGURE 3. EDX spectra of a)  $\text{TiO}_2$ , b)  $\text{Fe}_3\text{O}_4/\text{TiO}_2$  and c)  $\text{Ag}/\text{TiO}_2$

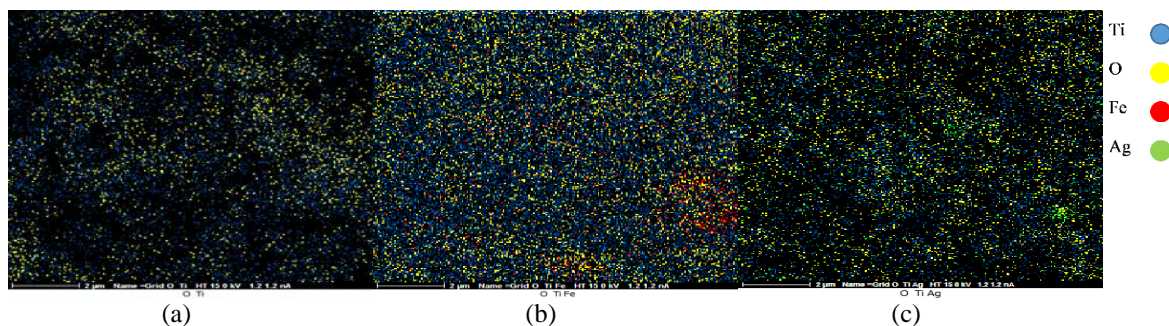


FIGURE 4. Elemental mapping of a)  $\text{TiO}_2$ , b)  $\text{Fe}_3\text{O}_4/\text{TiO}_2$  and c)  $\text{Ag}/\text{TiO}_2$

TABLE 2. Elemental chemical analysis of the prepared samples.

Sample	C wt%	N wt%	O wt%	Ti wt%	Fe wt%	Ag wt%
$\text{TiO}_2$	8.12	14.24	41.68	35.96	-	-
$\text{Fe}_3\text{O}_4/\text{TiO}_2$	6.31	9.80	40.15	41.99	1.75	-
$\text{Ag}/\text{TiO}_2$	10.26	12.43	37.12	36.13	-	4.06

The EDX result confirms the presence of C, Ti, O, Fe, Ag and N elements in these samples. In the EDX spectra of  $\text{Ag}/\text{TiO}_2$  sample, the absorption peak at 3 keV is for metallic silver and confirms the presence of silver nanoparticles in the prepared sample. Figure 4 shows elemental mapping images of the prepared samples.

### DRS analysis

The diffuse reflectance spectra of the prepared samples over the wavelength range of 200–800 nm are shown in Fig. 5. A. The DR spectrum of pure  $\text{TiO}_2$  consists of a broad intense absorption around 400 nm, due to the charge-transfer from the valence band formed by 2p orbitals of the oxide anions to the conduction band formed by 3d  $t_{2g}$  orbitals of the  $\text{Ti}^{4+}$  cations [11]. We calculated the band gap energy from the DR spectra according to below equation [12] for the prepared samples.

$$[F(R)hv]^{0.5} = A(hv - E_g)$$

Where A is constant, F(R) is the Kubelka-Munk function and  $E_g$  is the band gap. The band gap of the binary nanocomposites decreased slightly compared with  $TiO_2$  (Table 3).

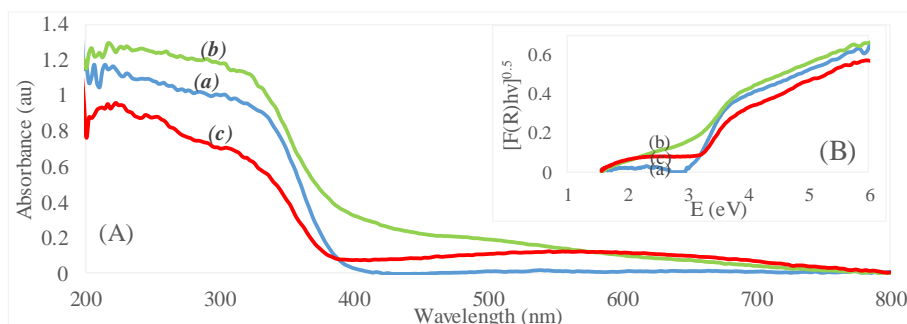


**FIGURE 5.** A): Diffuse reflectance spectra and B) Kubelka-Munk plots for the band gap energy calculation of a)  $TiO_2$ , b)  $Fe_3O_4/TiO_2$  and c)  $Ag/TiO_2$

**TABLE 3.** Band gap energy of the prepared samples.

Sample	$TiO_2$	$Fe_3O_4/TiO_2$	$Ag/TiO_2$
$E_g$ (eV)	3.05	2.70	3.02

### Photocatalytic performance of the prepared samples

To evaluate the photocatalytic activity of the synthesized samples a set of experiments for 2,4-DCP degradation with an initial concentration of  $40 \text{ mg L}^{-1}$  under visible light and UV irradiation at room temperature was carried out in aqueous suspension using  $TiO_2$ ,  $Fe_3O_4/TiO_2$  and  $Ag/TiO_2$  catalysts, and the experimental results are shown in Fig. 6. The experimental results demonstrated that among the prepared samples, the  $Ag/TiO_2$  catalyst showed the highest efficiency of the 2, 4-DCP degradation under visible light (42.40% degradation obtained after 180 min irradiation). The results show that the photocatalytic activity of pure  $TiO_2$  is lower than that of  $Fe_3O_4/TiO_2$  and  $Ag/TiO_2$  samples. It implies that the Ag dopant promotes the charge pair separation efficiency for  $TiO_2$  catalysts. The electron transfer from the  $TiO_2$  conduction band to Ag particles at the interface is thermodynamically possible because the Fermi level of  $TiO_2$  is higher than that of Ag metal. This results in the formation of a Schottky barrier at metal semiconductor contact region and improves the photocatalytic activity of  $TiO_2$ . The photocatalytic activity of  $Fe_3O_4/TiO_2$  sample is lower than pure  $TiO_2$  under UV irradiation implying that a stronger screen effect exists in our  $Fe_3O_4/TiO_2$  sample as compared with pure  $TiO_2$ . The  $Fe_3O_4$  NPs may be screened and weaken the UV irradiation needed to irradiate the  $TiO_2$  NPs in the  $Fe_3O_4/TiO_2$  sample [13] because, i)  $Fe_3O_4$  particles blocked some of the  $TiO_2$  active sites and ii) some UV irradiation was absorbed by  $Fe_3O_4$  particles.

### CONCLUSION

Pure  $TiO_2$  and binary nanocomposites of  $Fe_3O_4/TiO_2$  and  $Ag/TiO_2$  were synthesized by the sol-gel method for degradation of 2, 4-dichlorophenol and characterized by several techniques successfully. From among all of the samples only anatase phase was confirmed from the XRD results. The presence of Ag, Fe, O, and Ti atoms in the synthesized nanocomposites was confirmed by SEM/EDX. Among all samples,  $Ag/TiO_2$  catalyst exhibited the highest photocatalytic activity by 42.40 % degradation under visible light and 71.50 % degradation under UV irradiation after 180 min of irradiation.

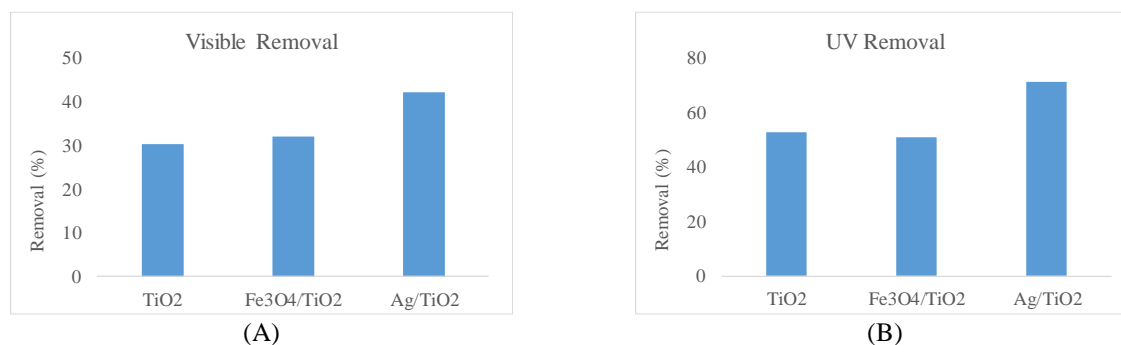


**FIGURE 6.** Photocatalytic degradation of 2, 4-DCP in the presence of the prepared samples under (A) visible light and (B) UV irradiation. Initial concentration of 2, 4-DCP, 40 mg /L; volume, 100 mL; catalyst dosage: 10 mg.

## ACKNOWLEDGEMENTS

The authors wish to acknowledge the financial support of University of Tehran for supporting of this research.

## REFERENCES

- [1] S. Oros-Ruiz, R. Zanella, and B. Prado, "Photocatalytic degradation of trimethoprim by metallic nanoparticles supported on TiO<sub>2</sub>-P25," *Journal of hazardous materials*, vol. 263, pp. 28-35, 2013.
- [2] Y. Tian and T. Tatsuma, "Mechanisms and applications of plasmon-induced charge separation at TiO<sub>2</sub> films loaded with gold nanoparticles," *Journal of the American Chemical Society*, vol. 127, no. 20, pp. 7632-7637, 2005.
- [3] M. Cao, P. Wang, Y. Ao, C. Wang, J. Hou, and J. Qian, "Photocatalytic degradation of tetrabromobisphenol A by a magnetically separable graphene-TiO<sub>2</sub> composite photocatalyst: mechanism and intermediates analysis," *Chemical Engineering Journal*, vol. 264, pp. 113-124, 2015.
- [4] A. E. Pirbazari, E. Saberikhah, and S. H. Kozani, "Fe<sub>3</sub>O<sub>4</sub>-wheat straw: preparation, characterization and its application for methylene blue adsorption," *Water Resources and Industry*, vol. 7, pp. 23-37, 2014.
- [5] C. H. Aguilar, T. Pandiyan, J. Arenas-Alatorre, and N. Singh, "Oxidation of phenols by TiO<sub>2</sub>/Fe<sub>3</sub>O<sub>4</sub> M (M= Ag or Au) hybrid composites under visible light," *Separation and Purification Technology*, vol. 149, pp. 265-278, 2015.
- [6] V. Mirkhani, S. Tangestaninejad, M. Moghadam, M. Habibi, and A. Rostami-Vartooni, "Photocatalytic Degradation of Azo Dyes Catalyzed by Ag Doped TiO<sub>2</sub> Photocatalyst," *Journal of the Iranian Chemical Society*, vol. 6, no. 3, 2009.
- [7] Z. Mo, C. Zhang, R. Guo, S. Meng, and J. Zhang, "Synthesis of Fe<sub>3</sub>O<sub>4</sub> nanoparticles using controlled ammonia vapor diffusion under ultrasonic irradiation," *Industrial & Engineering Chemistry Research*, vol. 50, no. 6, pp. 3534-3539, 2011.
- [8] A. Stoch, "Fly ash from coal combustion-characterization," Ms., Energy Engineering and Management, AGH University of Science and Technology, Kraków, Poland, 2015.
- [9] M. Khan and W. Cao, "Cationic (V, Y)-codoped TiO<sub>2</sub> with enhanced visible light induced photocatalytic activity: A combined experimental and theoretical study," *Journal of Applied Physics*, vol. 114, no. 18, p. 183514, 2013.
- [10] A. E. Pirbazari, P. Monazzam, and B. F. Kisomi, "Cobalt doped TiO<sub>2</sub> : Preparation, characterization and efficient degradation of methyl orange," presented at the International Conference on researches in Science and Engineering, Istanbul University, Turkey, 2016.
- [11] M. Hamadiani, A. Reisi-Vanani, and A. Majedi, "Sol-gel preparation and characterization of Co/TiO<sub>2</sub> nanoparticles: application to the degradation of methyl orange," *Journal of the Iranian Chemical Society*, vol. 7, no. 1, pp. S52-S58, 2010.
- [12] S. Kumar, S. Khanchandani, M. Thirumal, and A. K. Ganguli, "Achieving enhanced visible-light-driven photocatalysis using type-II NaNbO<sub>3</sub>/CdS core/shell heterostructures," *ACS applied materials & interfaces*, vol. 6, no. 15, pp. 13221-13233, 2014.
- [13] Y. Lin *et al.*, "Ternary graphene-TiO<sub>2</sub>-Fe<sub>3</sub>O<sub>4</sub> nanocomposite as a recyclable photocatalyst with enhanced durability," *European Journal of Inorganic Chemistry*, vol. 2012, no. 28, pp. 4439-4444, 2012.